Peptide Formation on Layered Mineral Surfaces: The Key Role of Brucite-like Minerals on the Enhanced Formation of Alanine Dipeptides

Journal:	*ACS Earth and Space Chemistry*
Manuscript ID	sp-2018-000523.R1
Manuscript Type:	Article
Date Submitted by the Author:	22-Jun-2018
Complete List of Authors:	Gregoire, Brian; Institut de Chimie des Milieux et Materiaux de Poitiers, Greenwell, Hugh; Durham University, Earth Sciences Fraser, Donald; University of Oxford, Department of Earth Sciences

Peptide Formation on Layered Mineral Surfaces: The Key Role of Brucite-like Minerals on the Enhanced Formation of Alanine Dipeptides

Brian Grégoire*,[a,c] H.Christopher Greenwell,[b] and Donald G. Fraser*,[a]

[a] Department of Earth Sciences, University of Oxford, South Parks Road, Oxford, OX1 3AN, United Kingdom.

[b] Department of Earth Sciences, Durham University, South Road, Durham, DH1 3LE United Kingdom.

[c] Université de Poitiers, CNRS, UMR 7285 IC2MP, 5 rue Albert Turpain, TSA 51106, 86073 Poitiers Cedex 9, France

E-mail : brian.gregoire@univ-poitiers.fr; don@earth.ox.ac.uk

Keywords : Layered double hydroxides, salt induced peptides formation, amino acids, Bernal's hypothesis, surface polymerization.

Abstract

Alkaline hydrothermal vent environments have gained much attention as potential sites for abiotic synthesis of a range of organic molecules. However the key process of peptide formation has generally been undertaken at lower pH, and using dissolved copper ions to enhance selectivity and reactivity. Here, we explore whether layered precipitate minerals, abundant at alkaline hydrothermal systems, can promote peptide bond formation for surface-bound alanine under cycles of wetting and drying. While we find low level activity in brucite and binary layered double hydroxide carbonate minerals (typically < 0.1% yield), the inclusion of structural copper to form a ternary layered double hydroxide mineral significantly increased the yield to > 7 %. However the performance decreased over successive wetting/drying cycles. Control experiments show that this high degree of dipeptide formation cannot be attributed to leached copper from the mineral structure. While only dipeptides are

observed, the yields obtained suggest that such processes, if occurring on the early Earth, could have added to the pool of available biological building units.

I. Introduction

One of the prerequisite conditions for the emergence of life on Earth by the formation of more complex systems from simpler organic precursors, would have been the presence of a stable liquid hydrosphere in which simple endogenic or exogenic organic compounds may interact to form more complex systems. Along with the formation of fatty acids, sugars and other protobiomolecules, a key step in such hypothesised processes is the formation of short chained peptides from simple amino acids [1].

While genetic information is carried and transferred by deoxyribonucleic acid (DNA) and ribonucleic acid (RNA), RNA may also act as a catalyst for biochemical reactions including autocatalysis. This led to the general proposal that life could have started using RNA –the so-called RNA World hypothesis [2, 3]. Although activated RNA nucleobases can be polymerized in the presence of montmorillonite [4-6], and RNA nucleotides are able to self-organize [7], RNA molecules themselves are relatively unstable [8] and only a few long RNA sequences may exhibit catalytic activity [9]. From a geochemical perspective, the formation of nucleobases, nucleosides and nucleotides involves concentrations of chemicals that are difficult to achieve in terms of our present understanding of likely prebiotic Earth chemistry [10, 11]. Unlike RNA, amino acids are known to form readily in experiments replicating putative reducing early Earth atmospheres [12] and are present in significant concentrations in carbonaceous chondrite meteorites [13, 14], indicating exogenic synthesis as well. Moreover, peptides and proteins exhibit enhanced catalytic properties and stability relative to RNA [15]. The formation of peptides from amino acids has already been demonstrated by Rode and co-workers using the salt-induced peptide formation (SIPF) reactions [16]. In SIPF, the amino acids condense in the presence of concentrated sodium chloride solutions and form peptide bonds to yield di-peptides and oligopeptides. The presence of dissolved copper cations leads to increased yields and selectivity [17]. The SIPF reactions exhibit interesting properties in a pre-

biological context, including regio-selectivity toward *alpha*-amino acids, and also enantioselectivity toward the L-forms of some amino acids [17-19]. Although glycine can polymerise up to Gly_6, the SIPF reaction usually forms only small peptides, generally limited to AA_2 or AA_3 where AA is an amino acid. However, on the early Earth, these small peptides may have undergone further evolution pathways via chain elongation and stabilisation on mineral surfaces [20]. Peptide formation can also be catalysed on mineral surfaces or edges as illustrated on montmorillonite, kaolinite and Fe(II) rich smectite [20-24]. However, the yield is low (typically less than 1% reaction yields for 5 wetting/drying cycles), and these reactions appear unlikely as a major contributor to the prebiotic formation of peptides from amino acids. Aside the wetting/drying cycles as driving force for peptide formation, thermal activation may also be suggested as an complementary way for producing peptides. Studies reported peptide formation over silica, Fe-oxides and metal-oxides with yield reaching 10-20% in some cases at relatively low thermal activation (60-120°C)[25-27]. Although less relevant in the context of prebiotic chemistry, high temperature thermal copolymerization or vapor phase amino-acid deposition on SiO_2 and TiO_2 have produced longer peptides that presents secondary structure, that may be considered as a crucial step in the path leading to living cell [28, 29].

The SIPF reaction remains a possible mechanism although more investigations are needed to improve the peptide yield and the enantioselectivity under plausible prebiotic conditions. While copper is one of the most abundant transition metal ions in sea water [30], the anoxic state and estimated pH of the early ocean makes the availability of free Cu^{2+} more questionable [31, 32], and the concentrations required for SIPF are usually relatively high. Copper is readily removed from seawater, being sequestered by chelation, precipitation or adsorption onto other mineral surfaces. To achieve the required high salt concentration to drive condensation reactions and peptide bond formation, the SIPF reaction has been

postulated to have taken place in evaporation cycles in coastal lagoons or salt lakes, and subsequent wetting could have been achieved by incoming high tides, waves or rain in order to start the reaction again. Experimentally, simulated evaporation/wetting cycles achieve a higher rate of peptide bond formation than constant volume experiments with reflux cooler to prevent evaporation [33, 34].

Since the discovery of abiotic hydrocarbons and rich microbial activity in oceanic alkaline hydrothermal fields, the idea that life may have originated in alkaline surroundings has gained credence [35-38]. Sedimentology records and evidence of nitrogen isotope fractionation in the Tumbiana Formation may indicate that the occurrence of alkaline lakes was frequent in the Archean environment [39]. Present day alkaline lakes and alkaline hydrothermal vents are much more biologically productive than freshwater water systems, and may have been so in the past [40]. Elevated pH conditions also induce the precipitation of $CaCO_3$, which limits Ca^{2+} binding to phosphate thus aiding the formation of phosphate based polymers, as well as enhancing the polymerisation of HCN that can play a role in the abiotic formation of amino acids [41]. Hanczyc *et al.* reported that the formation of vesicles is facilitated in alkaline media, consistent with their work showing that the origin of life may have been compartmentalized in lipid membrane [42]. However, alkaline conditions are not compatible with the peptide- forming SIPF reactions. SIPF reactions require dissolved Cu^{2+} ions, whereas Cu^{2+} precipitates if the water pH is alkaline, or the water oxic, depending on temperature. Thus, in order to form peptide bonds abiotically, and under alkaline conditions, a different mechanism to that of the homogeneous SIPF reactions is required.

Among minerals formed in alkaline lakes and off-axis alkaline hydrothermal vents, $Mg(OH)_2$, i.e. brucite, can be abundant [43, 44]. The structure of brucite $Mg(OH)_2$ consists of magnesium ions octahedrally coordinated to hydroxide ions. These octahedral units form infinite edge-sharing layers with the hydroxide ions sitting perpendicular to the plane of

cations. The layers are stacked on top of one another to form a three dimensional structure [45]. The local geometry around the metal and the hydroxide ions are distorted. This distortion has been discussed from a molecular orbital point of view, and, based on unit cell parameters and bond distances, it has been suggested that all brucite-like layered structures, including layered double hydroxides, exhibit similar distortion, [46, 47]. Brucite can readily undergo mineral transformations through isomorphous substitution of Mg^{2+} by M^{3+} species during precipitation to form layered double hydroxides (LDHs), a family of layered minerals with high layer cationic charge [48, 49]. Moreover, LDHs would have formed on the early Earth as a result of seafloor weathering processes such as serpentinization, or by reaction with solutions with high salinities [50, 51]. Other cations such as Mn(II), Al(III), Fe(III), Fe(II), Ni(II) or Cu(II) may also be incorporated within the brucite-like structure [52] and LDHs are notable for their anion exchange and concentrating capacity [53]. The main group of LDH materials, as used here, are thus described by the formula: $[M^{II}_{1-x}M^{III}_{x}(OH)_2]\ (A^{n-})_{x/n}.mH_2O$, where M^{II} and M^{III} are di- and trivalent cations of similar radii, respectively, A^{n-} is an exchangeable interlayer anion with charge n, and x represents the $M^{II}/(M^{III}+M^{II})$ molar fraction.

The present study explores the possible role that may have been played by these layered hydroxide minerals in early Earth chemistry, leading to the formation of peptides. While the SIPF reaction required acidic conditions, the experimental conditions applied in this study are alkaline with pH values of 9-9.5, and, in particular, include experiments conducted even in the absence of dissolved Cu^{2+} species. To achieve textural and structural homogeneity, we used brucite starting materials that were iso-structurally modified to form various layered double hydroxides with different compositions. The materials studied here are all based on commonly shared octahedrally coordinated cation sheets, and the results presented may thus possibly be extended to other minerals sharing similar structures. Peptide formation was followed in all cases using alanine monomers, on the basis of data from

molecular simulations reported in our previous work suggesting preferred reactivity of this amino acid at layered mineral interfaces [54].

2. Material and methods

2.1. Reagents

The cation providing salts ($MgCl_2$ $6H_2O$, $AlCl_3.6H_2O$ and $CuCl_2.2H_2O$) and the carbonate (Na_2CO_3) used for the preparation of the LDH and brucite phases were supplied by Sigma Aldrich and used as received. L-Alanine and D-Alanine amino acids were supplied by Sigma Aldrich and the dipeptide standard L-Ala-Ala was supplied by Bachem AG, Switzerland. An achiral high pressure liquid chromatography (HPLC) column was used so that no D-Ala-Ala was required. The ion-pairing reagent, sodium *n*-hexanesulfonate monohydrate, NaCl, KH_2PO_4 and concentrated phosphoric acid (50 wt.%) were also provided by Sigma Aldrich.

2.2. Synthesis of mineral phases

Synthesis of brucite: A 1 M NaOH solution was added dropwise (0.3 mL/min) to 50 mL of a 0.4 M solution of $MgCl_2$ dissolved in water. The reaction was stopped when the pH of the solution reached pH 12. The solution was then allowed to stir for 2 hours. Un-reacted salts were removed from the solution by multiple washing/centrifugation steps.

Synthesis of layered double hydroxides: Layered double hydroxides (LDHs) were prepared by the precipitation at low supersaturation method. The co-precipitation reaction was performed by the constant addition (0.3 mL/min) of a 0.4 M solution containing the divalent (Mg^{II}, Zn^{II}, Cu^{II}, Ni^{II}) and trivalent cations (Al^{III}) in the desired ratio into a solution of 0.25 M Na_2CO_3. The pH was maintained at 10 for all preparations by the simultaneous addition of a 1 M NaOH solution. Once the co-precipitation reaction was achieved, the slurries were vigorously

stirred for 2 hours. Then, the solution was centrifuged and thoroughly washed with water. The slurries were then dried in an oven at 60 °C overnight.

2.3. Salt induced peptide formation experiments

To allow comparison of the efficiency of LDH minerals for peptide bond formation, a set of controls using homogeneous SIPF reactions was first performed. Concentrations of alanine, copper and chloride were 100 mM, 50 mM and 400 mM, respectively. According to previous work a ratio AA:Cu of 2:1 was the most effective for optimising the SIPF reaction efficiency [52]. Experiments were performed over a period of 14 days, corresponding to 14 wetting/drying cycles. At selected intervals, solutions were sampled, analysed by HPLC, and the quantity of di-alanine peptides formed was measured. Both L-Alanine and D-Alanine were used as starting reactants, in order to measure possible enantioselectivity.

2.4. Evaporation cycle experiments

Homogeneous SIPF experiments The formation of peptide bonds was carried out in drying and wetting cycle experiments that simulate the environment in tidal lagoons ion a primordial Earth. A classical SIPF experiments was first performed serving as a reference to assess the influence of LDH chemistry on peptide yield formation and enantioselectivity. The SIPF solution consisting of 500 mM NaCl and 40 mM CuCl2 was used with a starting solution of 100 mM of L or D Alanine. After mixing, 1 mL aliquots of the reaction solution were transferred into 2 mL Eppendorf® and then held in a thermostatic oven at 80°C to start the first evaporation cycle within 24h. After each cycle, 1 mL of ultrapure water was added to the residue for the next cycle under the same conditions. After 0, 1, 4, 7 and 14 cycles, the evaporated sample were removed and frozen dry at -20°C for further analyses.

Reactions in the presence of brucite and LDH minerals In order to investigate the role of the chemical composition of LDHs involved in peptide formation and the possibility that minerals

can advantageously replace Cu^{2+}, a very similar protocole as that of the SIPF reaction was adopted. An aliquot of 1 mL of a solution containing 500 mM NaCl and 100 mM of L or D Alanine was contacted with 0.45 mmol of the materials investigated. Since the chemical composition of the solid phases was the studied parameter, the mass of the materials was adjusted to fit the required molar quantity. This allows the efficiency of the catalyst to be directly compared through the observed conversion. The conditions of the wetting-and-drying cycle was identical as that of the SIPF reaction described above. For the sake of completeness, one experiment was carried out by contacted the SIPF reagents with LDH.

2.4. Characterisation methods

Powder X-ray diffraction (XRD). Patterns were recorded with a Phillips X'Pert Pro MPD diffractometer at Oxford University in reflection geometry using Cu Kα1 radiation (λ = 1.5406 Å). Samples were finely ground and continuously rotated to improve statistics. The 2θ range was between 5–70 ° with a step size of 0.01671 ° and a scan time per step set at 2 s giving a scan rate of 2 °/min. The cell parameters were determined from peak profile analysis using pseudo-Voigt functions [55].

Raman spectroscopy. The Raman analyses were performed on a Jobin Yvon T64000 equipped with nitrogen cooled Charged Coupled Device detector and a motorized XYZ stage in the University of Oxford. The samples were placed on a glass holder and mounted in the focal plane of an Olympus X50 objective (N.A = 0.55). The spot area was around 2 μm². A 514.53 nm exciting radiation was used and the power was adjusted depending on the nature of the samples to prevent sample degradation. The spectral resolution was about 4 cm^{-1} and the precision on the wavenumber was lower than 1 cm^{-1}.

High performance liquid chromatography analysis. After a certain number of cycles, the residues were dissolved again, filtered and analysed by reverse-phase ion-pairing chromatography on a Waters 600s system, equipped with a diode array detector. Quantitative

and qualitative results were obtained by comparing the retention time, the response factor and the UV spectra of standard alanine references. Depending on the quantity of dipeptide in the solution, 2 µL to 10 µL of the sample solutions were injected into a Waters ODS column (5 µm, 4.6 x 250 mm) equipped with a 20 mm pre-column of the same materials. The analyses were performed in isocratic mode with a mobile phase containing 50 mM KH_2PO_4 and 7.5 mM *n*-$C_6H_{13}SO_3Na$ in ultrapure water, adjusted to pH 2.3 with concentrated H_3PO_4. The UV/Vis detector was set at 200 nm. Two injections per run were performed.

3. Results and Discussion

In this section, we first report and discuss the structure of the starting mineral phases prepared. The simple hydroxide ($Mg(OH)_2$), binary layered double hydroxides (Mg/Al, Ni/Al and Zn/Al) and ternary layered double hydroxides (Mg/Cu/Al) are described in turn. Though care was taken to obtain materials of similar crystallinity to ensure reasonable comparison between peptide forming reactions, as shall be seen, variations were noted as a function of composition of the layered material. Having understood the variation in mineral structure, the activity of each system with respect to peptide bond formation is then explored.

3.1. Structural characterisation of mineral phases

Simple and binary phases - brucite to layered double hydroxides. The XRD pattern of brucite ($Mg(OH)_2$) is displayed in **Figure 1a** and indexed with a hexagonal symmetry (P-3m1) space group. The cell parameters were determined as a = 3.140 Å and c = 4.732 Å, matching reported cell parameters [45]. Carbonate was chosen as the LDH interlayer anion, as the most plausible in alkaline water [56] and Al^{3+} is the trivalent cation. **Figure 1a** also displays the XRD pattern of Mg_2Al and Mg_3Al LDH phases to identify the role of Mg content on the reactivity. This comparison is enabled by the fact that the presence of carbonate anions prevents any interlayer reactivity so that only surface sites are accessible. Lowering the layer charge

density (lower Al^{3+} content) leads to an increase in the interlayer spacing (shift toward lower diffraction angle) as a result of the decrease of the electrostatic interaction between the positive charge in the layer and the negative charge in the interlayer domain. The *a* parameter also increases with decreasing layer charge density. Since the cell parameters evolve linearly with the layer charge density, these two parameters *a* and *c* can be good indicators of the successful control of the cation ratio within the LDH layers [57]. Different divalent cations were also considered including Mg^{2+}, Ni^{2+}, and Zn^{2+}; all these cations being present in the early ocean [58]. XRD patterns of the M^{II}-Al^{III} LDH phases synthesised are presented in **Figure 1b**. Since the synthesised LDHs were prepared with a unique layer charge density and interlayer anion, the *c* parameter ($c = 3/2(d_{003} + 2d_{006})$) does not change (as shown in **Table 1**). The position of the (110) XRD peaks enables calculation of the ***a*** parameter, which can be correlated with the cation-cation distance. This parameter is cation dependent, varying with the ionic radii of the cations at a given cation ratio [59].

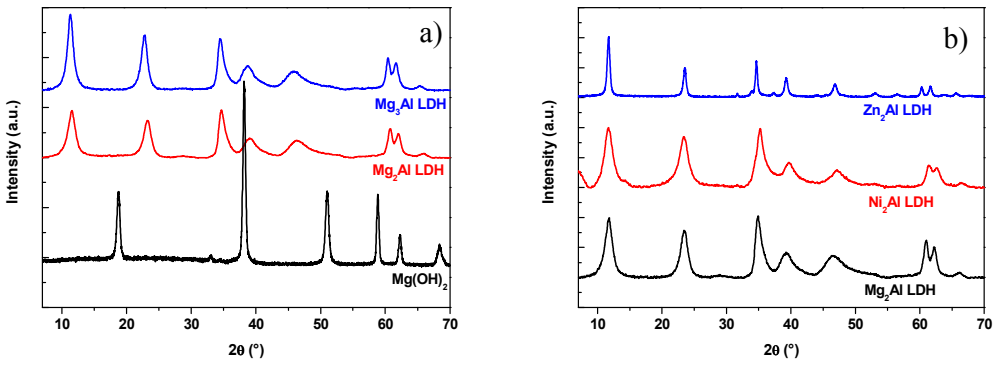

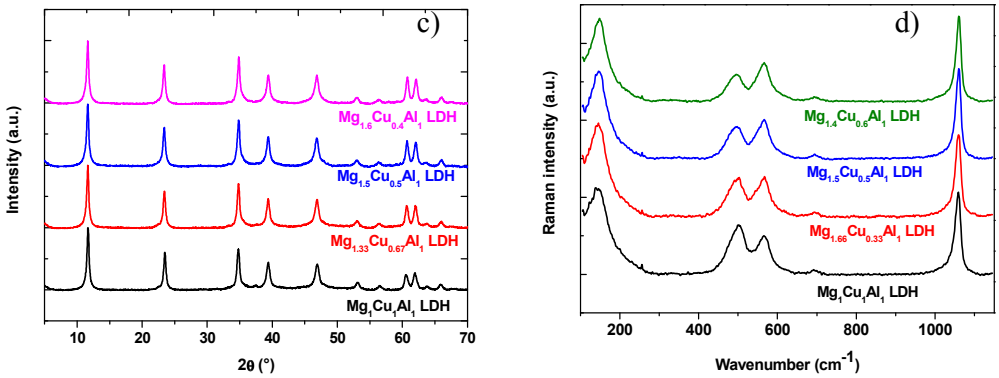

Figure 1. Powder X-ray diffraction patterns for minerals prepared in this study: (a) comparing the effect of Mg content in layered minerals. (b) comparing the effect of the nature of the divalent M^{II} = Mg^{II}, Ni^{II}, Zn^{II} in layered double hydroxides (c) Ternary layered double hydroxides with M^{II}:M^{III} = 2 and different Cu^{II} content. The corresponding Raman spectra of these ternary phases are displayed in (d).

Although similar synthesis methods were used, there is a variation in crystallinity that depends on the cationic composition and stoichiometry. The apparent domain size, calculated with the Scherrer equation (K = 1), along the [001] direction corresponds to the average thickness of the crystallites, while the apparent domain size along the [110] direction allows the apparent diameter of LDH crystals to be estimated. The domain size along the [110] direction is higher than that along the [001] direction as a result of the classical platelet-like morphology observed for LDH particles prepared by co-precipitation [57] (**Table 1 and Table ESI 1**). Interestingly, the nature of the cations dictates the crystallinity of the LDH phases. Among all the cation couples used, Zn_2Al exhibits much larger coherent domain size in both directions. This enables investigation of whether the cations or the textural properties play the major role in the reactivity of these phases.

Ternary Layered Double Hydroxides To investigate the possible role of incorporating Cu in LDHs, ternary Mg/Cu/Al LDH materials were also prepared. **Figure 1c** shows the XRD

patterns of the ternary $Mg_{2-y}Cu_yAl$ LDH phases. All XRD peaks can be indexed in the common R-3m group of LDH, indicating the samples are phase pure. The symmetry of the XRD lines suggests a regular stacking sequence, as expected when carbonate is intercalated [60]. The positions of the (00l) and (110) XRD lines were used to calculate the cell crystallographic parameters. Since the XRD lines exhibit quite uniform broadening, the apparent diameter along the [001] direction and along the [100] direction can also be calculated [61]. These values are reported in **Table 1**.

Variation of the cell parameters with changing Cu^{2+} content gives direct evidence of the incorporation of the copper ions within the brucite-like sheet. The overall layer charge density of the ternary system is constant and the ***c*** parameter did not vary. In contrast, the unit cell ***a*** parameter increased with increasing copper content through the replacement of smaller Mg^{2+} ions by larger Cu^{2+} ions. From the domain size indicated by the Scherrer equation, it can be seen that the Cu^{2+} content has a negligible effect on the apparent domain size along the [00l] direction, i.e. thickness of crystallite, but a significant effect on the apparent domain size along the [110] direction i.e. the basal plane of the crystallites. This may be explained by octahedral Jahn-Teller distortion related to the presence of octahedral Cu^{2+} ions. The coherent domain size decreases as the Cu^{2+} content increases.

Table 1. Cell parameters and calculated domain sizes for the prepared ternary Mg/Cu/Al layered double hydroxide minerals. The error on the determination of cell parameters was estimated at 0.03%.

LDH	Cell parameters (Å)		Apparent domain size (nm)	
	c (Å)	a (Å)	along [001]	along [110]
$Mg_1Cu_1Al_1$ LDH	22.824	3.054	22.8	33.1
$Mg_{1.33}Cu_{0.66}Al_1$ LDH	22.819	3.050	22.2	42.7
$Mg_{1.5}Cu_{0.5}Al_1$ LDH	22.823	3.048	21.5	46.2
$Mg_{1.6}Cu_{0.4}Al_1$	22.824	3.046	21.3	48.8

Mg_2Al	22.684	3.037	7.9	23.6

To ensure that Cu^{2+} had been incorporated within the LDH layer, and not precipitated as another phase, Raman spectra were obtained (**Figure 1d**). Raman spectroscopy probes local structure, rather than the long-range structure characterised by XRD, and has the advantage of being able to detect even poorly crystallised phases. The Raman bands located at 1056 cm^{-1} and 680 cm^{-1} correspond to the symmetric stretching and bending modes of the carbonate anion respectively. At lower wavenumbers, an intense band at around 120 cm^{-1} is attributed to translational mode of the interlayer species [62]. The two bands situated at 500 cm^{-1} and 560 cm^{-1} are assigned to the LDH phase as reported elsewhere [63]. No other band is observed in this spectral range, confirming that the LDH prepared are phase pure and no second Cu^{2+} phase is present.

Interestingly, the positions of the LDH bands are the same even when the proportion of Cu^{2+} in the sheet is varied, indicating that the intralayer bonding is similar in all cases. However, the relative intensities of the two bands present at 560 cm^{-1} and 500 cm^{-1} show systematic changes reflecting the content of the Cu^{2+} ions (**Figure ESI 2)**. By analogy with binary Mg_2Al LDHs, where the most intense band is located at 560 cm^{-1}, the Raman band situated at 560 cm^{-1} is attributed to the Mg_2AlOH domain, with the one at 500 cm^{-1} assigned to the Cu_2AlOH domain, suggesting cations in the ternary systems may form distinct domains. A similar interpretation was proposed by Leroux *et al.* on systems of the type CoCuAl on the basis of EXAFS spectroscopy [64].

3.2 Salt induced peptide formation experiments

The results obtained for the control experiments with no LDH present, and using salt induced peptide formation (SIPF), are shown in **Figure 2**. The conversion yields are expressed as percentages of the initial amino acid concentration. Both curves are very similar, irrespective

of the chirality of the amino acid. A net increase is observed until the fourth cycle, and then the quantity of peptide formed decreases with increasing number of cycles. This may reflect formation of dipeptides followed by hydrolysis, degradation or competition of alanine with the dipeptide for the catalyst site. Formation of higher molecular weight peptides by oligomerisation reactions of the dipeptides has not been observed in these systems. Any enantioselectivity of the SIPF reaction is not obvious under our experimental conditions. Rode and Suwannachot reported that the initial concentration of amino acid determines the extent of enantioselectivity [65]. A slight enantioselectivity toward the L form is observed after the first four cycles, as the dipeptide yield decreases, but the statistical significance of this result is questionable. These SIPF syntheses were repeated with different cation configurations. Repetition of the simple SIPF reaction after removing either Cu^{2+} or NaCl, or on changing the nature of the divalent cation (Ni^{2+}, Zn^{2+} or Mg^{2+}) resulted in no detectable amounts of di-peptides.

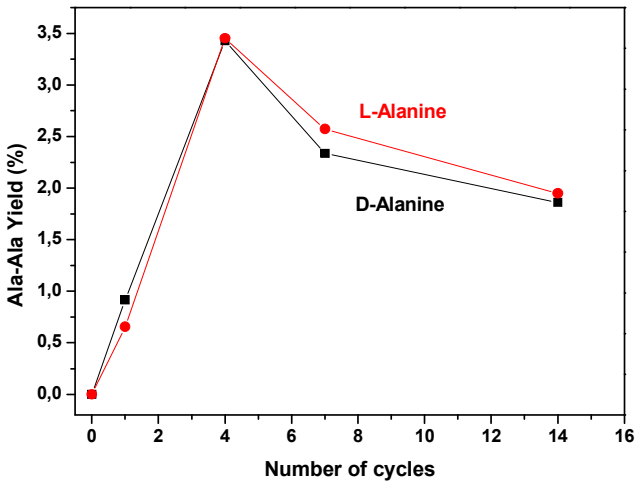

Figure 2. Salt induced peptide formation reaction yields of di-alanine (L and D) is plotted versus number of wetting/drying cycles.

3.3 Mineral induced peptide formation experiments

Brucite and binary layered double hydroxide minerals The results of peptide forming experiments for different LDH compositions are shown in **Figure 3**. The four curves all show a continuous increase in peptide formation over the entire number of wetting/drying cycles in contrast to the behaviour observed in the homogeneous SIPF reaction (**Figure 2**). This suggests that the LDH surface stabilizes or protects dipeptides against subsequent hydrolysis more efficiently than the SIPF reaction. After 14 cycles, the peptide yield reaches 0.10% for Mg_2Al LDH, 0.06% for $Mg(OH)_2$, 0.03% for Zn_2Al LDH and less than 0.01% for Ni_2Al LDH. These values are much lower than those obtained from the homogeneous SIPF reactions. Note that the pH of the starting solution in contact with the solid catalyst was very similar in each case, because of the strong buffering capacity of these carbonate materials, with values ranging from pH 9 to pH 9.5. Based on the values of the apparent domain size determined by XRD (Figure ESI 1), it is inferred that the crystal properties of Ni_2Al and Mg_2Al LDH are similar, suggesting that the difference of reactivity cannot be simply attributed to the accessibility of surface active sites and that the critical parameter is the nature of the cation. Since carbonate was the charge balancing anion, no anion exchange reactions would have occurred owing to the stability of carbonate LDHs, and only the exterior surfaces should be accessible to species in solution. In addition, though edge cations may be exposed, the cations in LDHs are mainly located in the centres of hydroxide octahedra, and are therefore not readily accessible for bonding with solution amino acids. Interestingly, both Mg-based materials exhibit the higher conversion yield, showing that Mg-containing layers are the most reactive/stabilising for peptide formation.

The small conversion yield in all cases implies that most of the surface sites do not participate in the reaction, with only a small fraction of all surfaces sites being active, for example at structural defects or LDH particle edges. Interestingly, though the structures are

similar, $Mg(OH)_2$ and Mg_2Al LDHs exhibit substantially different reactivity for alanine dipeptide formation. Assuming a surface mechanism, the only sites that are accessible from solution are the hydroxide layers and, for the LDH, external bound carbonate anions. Peptide bond formation requires reaction at surface basic sites and, in LDH systems, the strength of the basic sites depends on the nature of the cations, particular in terms of electronegativity and the electron density gradient in the layers influencing the basicity of the hydroxyl group. The greater the electronegativity of the atom, the weaker the basic sites formed. In the LDH structure, and assuming cation ordering within the layer, all OH groups are similar, and all are bonded to two divalent cations and one trivalent cation (Mg_2Al-OH moieties) [66]. Since the only trivalent cation present was Al^{3+}, comparison of the electronegativities of the divalent cations between the various LDHs allows an estimation of the relative basicity of the different surfaces. The electronegativity of the cations follows Mg (1.31) < Zn (1.65) < Ni (1.91). These are in good accord with the respective peptide yields after 14 days. Among the LDHs tested, Mg based compositions with the most basic sites also gave the highest yields as expected.

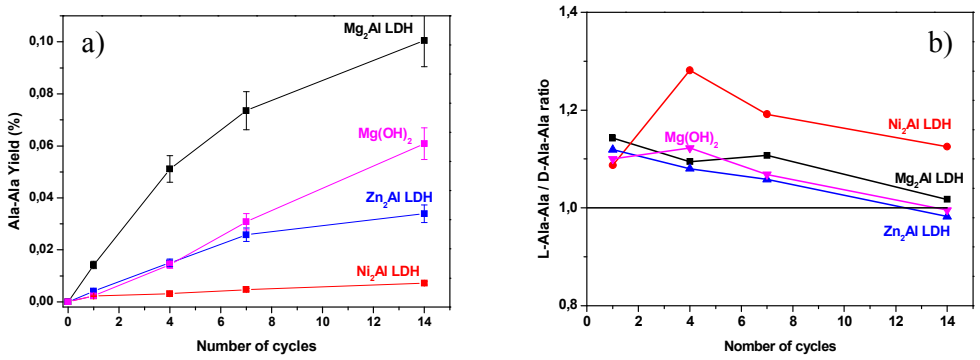

Figure 3. Results from peptide forming reactions on brucite and binary layered double hydroxides, where M^{2+} was either Mg, Zn or Ni, showing: (a) yields of di-alanine against the number of wetting/drying cycles; (b) the enantiomeric excess.

Influence of the layer charge density LDHs with different Mg:Al ratios were also prepared, along with $Mg(OH)_2$, and used to induce peptide formation. The experimental conditions were similar to those previously described. The results of these experiments are presented in **Figure 4a**. In each case a continuous increase in peptide yield is observed over the number of cycles, but the quantity of peptides formed depends on the layer charge density. After 14 cycles, the di-alanine yield reaches 0.1% for Mg_2Al LDH, 0.08% for Mg_3Al LDH and 0.06% for $Mg(OH)_2$. These three materials exhibit higher peptide conversion yields than those with the other cations (Zn or Ni), pointing towards the potential role of the Mg materials, especially given their abundance at alkaline vents.

Compared with brucite, the presence of Al, with stronger electronegativity, slightly weakens the basicity of the surface sites which seems to have a positive influence on the reactivity. These results were not expected given the reasoning given above that increasing the basicity will promote peptides formation. This apparent discrepancy suggests that the strength of the basic sites does not provide a complete rationalization for interpreting the actual yield of peptide formation when brucite and LDH materials are compared. Moreover, as observed in table S1, the apparent domain size of brucite and LDH materials are largely different, so that the number of active sites for peptides reaction is believed to be different. As far as Mg_3Al LDH is concerned and assuming an ordered distribution of the cations within the layer, OH groups can be linked to three magnesium (25%) or two magnesium and one aluminum (75%)[66]. As observed in figure 3a, the observed peptide yields is about 80% of the one of Mg_2Al LDH potentially indicating that the surface active sites may be $Mg_2Al(OH)$ moieties. Peptide bond formation involves nucleophilic attack of the amino group on the electrophilic carboxylate carbon. At pH 9-9.5, a significant population of the amino groups will be protonated, which decreases its nucleophilic character. Given that the point of zero charge LDH lies generally in the range [10.5 - 11.5][67-70], the LDH surface acquires a positive

charge at pH 9-9.5 that may be balanced by an increased concentration of OH^- near the surface of the particle. Therefore, the local pH at the surface of the particles may be much higher than the one in solution, enhancing the deprotonation of the amino group and promoting its nucleophilicity thus leading to a higher conversion yield.

Figure 4b shows the dipeptide ratio L-Ala-Ala/D-Ala-Ala over the number of cycles. Interestingly, slight enantioselectivity is observed with the L form being favoured, especially during the first cycle. With increasing number of cycles this enantiomeric excess disappears and could reflect different reactivity between L form and D form as reported for the SIPF reaction, or different surface adsorption properties.

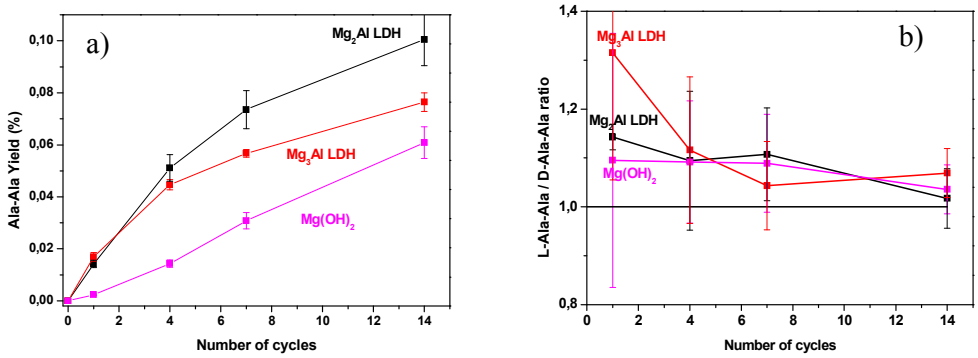

Figure 4. Results from peptide forming reactions on brucite and binary Mg/Al layered double hydroxides, where Mg^{2+}/Al^{3+} was either 2 or 3, showing: (a) yields of di-alanine against the number of wetting/drying cycles; (b) the enantiomeric excess.

3.4 Assessing the role of copper in mineral induced peptide formation experiments

Mg-based layered double hydroxides are shown above to be effective substrates for the formation of alanine peptides, even in the absence of Cu(II). However, compared with the homogeneous SIPF reaction, run as a comparison, the peptide yields were much lower, and therefore aqueous Cu(II) in the SIPF reaction is a better catalyst than either the LDHs or

brucite. To investigate whether Cu(II) can play a role in LDH –catalysed peptide synthesis, two sets of experiments were carried out.

Binary LDHs with soluble copper and SIPF reagents In the first set of experiments, the SIPF reaction and the LDH catalyst were combined and the simple SIPF reaction with the SIPF reactants (NaCl, Cu^{2+}, and Alanine) was carried out in the presence of Mg_2Al LDH. Under these conditions, no peptide was formed and it seems the LDH mineral surface inhibits the SIPF reaction. It is speculated that this is due to competition between the complexation reaction with the copper that is involved in the SIPF reaction and the surface adsorption sites on the minerals, thus preventing any SIPF reaction.

Ternary LDHs with structural copper In a second set of experiments, copper was instead directly incorporated into the LDH layers at various concentrations to determine if structural copper promotes the formation of peptides. The results, given in **Figure 5a**, show that the presence of structural Cu(II) in the LDH significantly increases the conversion yield from 0.1% in the binary system to values that range from 2.5% - 7% in the ternary system, a remarkable increase. The profiles of the curves are similar in all these phases and show a continued increase in the conversion to peptides over the number of cycles. Moreover, a linear correlation is observed between the quantity of Di-Ala formed after 14 days and the initial quantity of copper in the layer (**Figure ESI 3**). Unlike binary LDHs, the peptide formation reaction in the ternary system exhibits slight enantioselectivity toward the D-amino acids, the extent of which is correlated with the quantity of copper within the layer **(Figure 5b)**. The reason for this remains unclear.

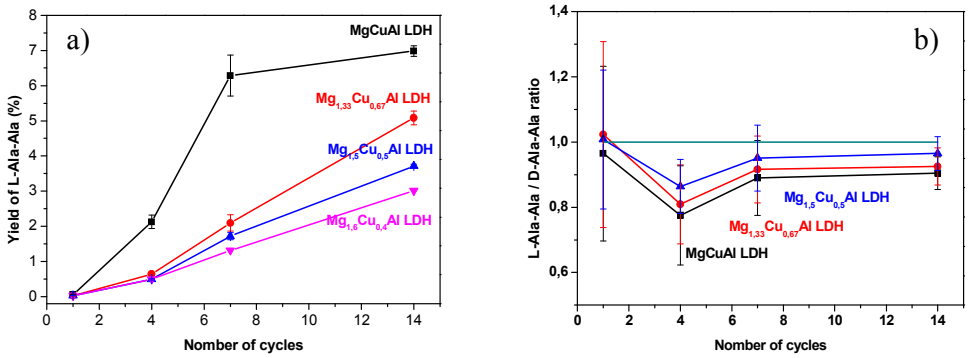

Figure 5. Results from peptide forming reactions on ternary Mg/Cu/Al layered double hydroxide minerals, with varying Cu^{2+} content, showing: (a) yields of di-alanine against the number of wetting/drying cycles for each mineral; (b) the enantiomeric excess.

During the experiments, changes in the colour of the solution were observed, from a pale green of the ternary LDH system to a dark blue. This strongly suggests that copper was released into solution during the experiments. However, the combination of LDH and SIPF reagents in the initial experiment yielded no dipeptide, and also the higher yields than found in the SIPF reaction alone provide evidence that it is not the leached copper that induces the observed reactivity.

In order to gain more insight into this transformation, samples were taken at different stages of reaction and analysed by Raman spectroscopy. To ensure that the samples were homogeneous and that the results discussed relevant, spectra were recorded at 2 µm resolution on several different areas of each of the samples. Some differences were observed that could possibly be assigned to other phases but the band intensities and frequencies assigned to the LDH were seen to be highly reproducible wherever the signal were collected. It is clear from **Figure 6** that transformation of the LDH phase occurs with increasing number of cycles as shown by the decrease in intensity of the LDH bands at 500 cm^{-1}, while the band located at 560 cm^{-1} remains unchanged. The former band is assigned to Cu_2Al-OH groups while the

latter is attributed to Mg_2Al-OH groups in the ternary MgCuAl system. This spectral evolution may be correlated with the partial dissolution of the Cu_2Al domain. This interpretation is further supported by the visual resemblance between the LDH taken at the 14th cycles and Mg_2Al binary LDH phases and X-ray evidence below.

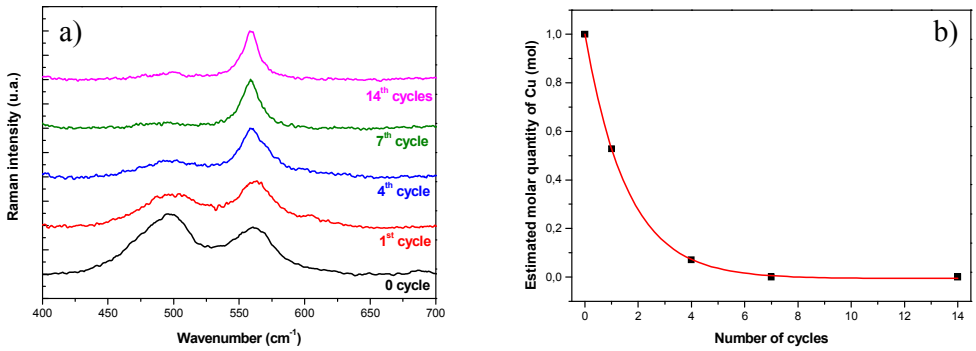

Figure 6. Change in the Raman spectra of MgCuAl LDH where Mg/Cu = 1 showing: (a) the peaks at 500 cm^{-1} and 560 cm^{-1} as a function of number of wetting cycles; (b) calculated residual LDH framework Cu^{2+}.

As observed in **Figure ESI 3**, a linear correlation was found between the quantity of copper within the LDH phase and the relative intensity of the Raman band. Through applying this correlation to the data from our samples, shown in **Figure 6a**, the quantity of structural LDH copper can be estimated. As can be seen from **Figure 6b**, the quantity of copper decreases exponentially over the number of cycles, to approach 0 after the 7th cycle. To explore this in more detail, the MgCuAl samples that underwent 14 days of wetting/drying cycles were analysed by XRD and compared with the pristine MgCuAl LDH phase (**Figure 7**). After 14 cycles, the layered structure is conserved as indicated by the typical LDH signature. The cell parameters are a = 3.036 Å and c = 22.716 Å. The c parameter is very slightly lower than that of the pristine sample suggesting that the layer charge density has almost been conserved. However, a more drastic decrease of the a-parameter suggests that the composition of the layer has changed significantly. The value of the a-parameter is very close to that Mg_2Al LDH, implying that most of the copper has escaped from the structure as deduced from

Raman analysis. This is further supported by the presence of new reflections shown by arrows on **Figure 7** and which may be assigned to Cu^{II} phases. It is interesting to note that the rehydration of the sample taken at the 14th cycle showed a complete resolubilisation of Cu^{II}, without any detection of deposited blue crystals at the bottom of the flask. Although the precipitation of $CuCl_2$ salt resulting from the drying process prior to XRD measurements may be suggested, the absence of direct evidence and the restricted number of XRD peaks make the determination of the Cu phase complicated.

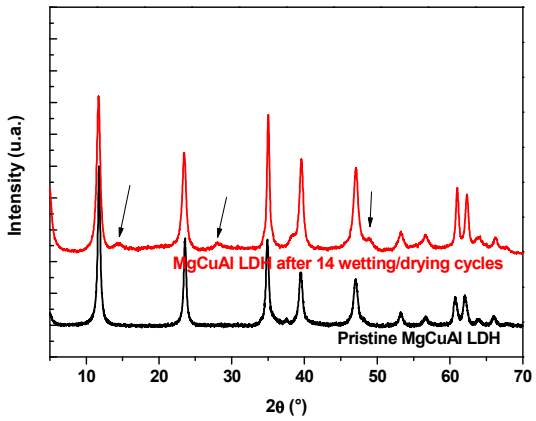

Figure 7. Powder X-ray diffraction patterns for the ternary MgCuAl layered double hydroxide before and after 14 wetting/drying cycles. Emergence of new peaks marked with arrows in the post-treatment X-ray diffraction pattern.

Catalyst recycling of ternary LDHs with structural copper In order to ensure that the non-LDH Cu^{II} phase was not involved in the formation of the peptides observed, new experiments were performed. MgCuAl LDH was first placed in a fresh solution containing the amino acid and NaCl. Once the solution was fully evaporated, the materials were rinsed thoroughly with water several times. Then, a new cycle was started by addition of the amino acid/NaCl solution. By comparison with the previous experiments, this corresponds to an evaluation of the efficiency (reusability) of the catalyst every cycle. The results are shown in Figure 8, and

the value of the di-alanine yield after the first cycle (0.057%) corresponds reasonably well with that determined in the first cycle of the previous experiments (0.065% in **Figure 5a**). A continuous decrease of the quantity of peptide then appears until the 6th cycles where a steady value of 0.03% is noted. The decrease of the efficiency may possibly be attributed to the mineralogical transformation of the LDH phase, decreasing the quantity of basic sites. The value of 0.03% is higher but relatively close to that obtained in the absence of Cu(II) with Mg_2Al LDH after the first cycle (i.e. 0.015%) , strengthening our hypothesis that after Cu release, the remaining solid material is Mg_2Al LDH. From the 6^{th} to the 14^{th} cycle, the quantity of peptides formed every cycles is identical, meaning that the binary LDH shows very good stability over time despite its low reactivity. These experiments confirm that the non-LDH Cu phase does not participate in the formation of peptides. Comparison of Figure 8 and Figure 5a, shows the key role of copper.

As reported above, no reaction was observed when copper and amino acid were both simply in contact with LDH in the combined SIPF/binary LDH experiments, and we speculate that this is the result of surface scavenging of Cu(II) from solution. In contrast, incorporation of Cu(II) in the solid LDH structure leads to high yields for amino acid-peptides conversion. This result is interesting since in solution with the simple SIPF reactions, high copper concentration is known to inhibit the formation of di-alanine [71]. This suggests that the reaction mechanism for di-alanine peptide formation in the presence of Cu-bearing MgAl LDHs may involve specific chemisorption of alanine on the Cu-LDH surface.

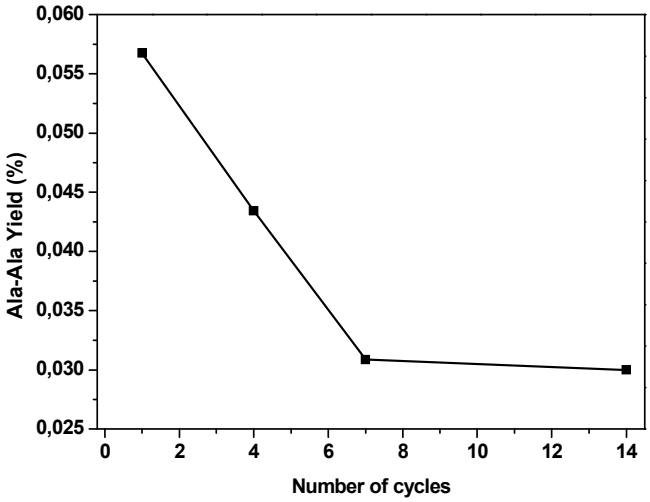

Figure 8. Di-alanine yield as a function of number of cycles for the MgCuAl system where the material was rinsed throughly between each wetting cycle.

4. Conclusions

This study set out to examine the possible role of layered precipitation minerals as catalysts for the formation of peptides in alkaline media under conditions related to early Earth hydrothermal vents. The results presented here suggest that among all brucite and binary layered double hydroxide structures tested, Mg-based materials exhibit better catalytic activity than those based on Ni or Zn. In addition, reusability tests suggest that their catalytic activity is conserved over time, so that a continuous supply of peptides may have been provided by these materials. The surface basicity may explain this reactivity of Mg-based materials through the activation of the amino group, thus strengthening its nucleophilic character. Incorporation of Cu within the brucite-like sheet enhances the reactivity more than 20 times to give dipeptide yields of up to 7% Though this high reactivity leads to a progressive dissolution of copper, under alkaline conditions we speculate that subsequent re-precipitation of the Cu within a new LDH would maintain the cycle of di-alanine formation.

5. Acknowledgements

The authors (BG, DGF, HCG) wish to acknowledge the Leverhulme Foundation (Grant RPG-2012-551) for the funding that enabled this work. BG and DGF would like to thank Phil Wiseman from the Chemistry Research Laboratory of the University of Oxford for giving access to XRD facilities.

6. Supporting informations

Cell parameters for various LDH composition, linear correlation to assess the Cu content in layered double hydroxides using Raman spectroscopies, and correlation between the dipeptide yield and the Cu content within the LDH layer.

References

(1) Nutman, A. P.; McGregor, V. R.; Friend, C. R. L.; Bennett, V. C.; Kinny, P. D., The Itsaq Gneiss Complex of southern West Greenland; the world's most extensive record of early crustal evolution (3900-3600 Ma). *Precambrian Research* **1996,** *78* (1–3), 1-39.

(2) Benner, S. A.; Kim, H.-J.; Yang, Z., Setting the Stage: The History, Chemistry, and Geobiology behind RNA. *Cold Spring Harbor Perspectives in Biology* **2012,** *4* (1).

(3) Robertson, M. P.; Joyce, G. F., The Origins of the RNA World. *Cold Spring Harbor Perspectives in Biology* **2012,** *4* (5).

(4) Ferris, J. P.; Hill, A. R., Jr.; Liu, R.; Orgel, L. E., Synthesis of long prebiotic oligomers on mineral surfaces. *Nature* **1996,** *381* (6577), 59-61.

(5) Ertem, G.; Ferris, J. P., Synthesis of RNA oligomers on heterogeneous templates. *Nature* **1996,** *379* (6562), 238-40.

(6) Ferris, J. P.; Ertem, G., Montmorillonite catalysis of RNA oligomer formation in aqueous solution. A model for the prebiotic formation of RNA. *J Am Chem Soc* **1993,** *115* (26), 12270-12275.

(7) Fraser, D. G.; Deak, D. S.; Liu, S.; Castell, M. R., Structure of vapour deposited adenine on a nanostructured perovskite surface studied by STM. *Faraday Discuss.* **2006,** *133* (0), 303-309.

(8) Vlassov, A.; Kazakov, S.; Johnston, B.; Landweber, L., The RNA World on Ice: A New Scenario for the Emergence of RNA Information. *J. Mol. Evol.* **2005,** *61* (2), 264-273.

(9) Wochner, A.; Attwater, J.; Coulson, A.; Holliger, P., Ribozyme-Catalyzed Transcription of an Active Ribozyme. *Science* **2011,** *332* (6026), 209-212.

(10) Sanchez, R. A.; Orgel, L. E., Studies in prebiotic synthesis: V. Synthesis and photoanomerization of pyrimidine nucleosides. *J. Mol. Biol.* **1970,** *47* (3), 531-543.

(11) Powner, M. W.; Gerland, B.; Sutherland, J. D., Synthesis of activated pyrimidine ribonucleotides in prebiotically plausible conditions. *Nature* **2009,** *459* (7244), 239-242.

(12) Miller, S. L.; Urey, H. C., Organic Compound Synthesis on the Primitive Earth. *Science* **1959,** *130* (3370), 245-251.

(13) Cronin, J. R.; Pizzarello, S., Amino acids in meteorites. *Adv. Space Res.* **1983,** *3* (9), 5-18.

(14) Glavin, D. P.; Dworkin, J. P., Enrichment of the amino acid l-isovaline by aqueous alteration on CI and CM meteorite parent bodies. *Proceedings of the National Academy of Sciences* **2009,** *106* (14), 5487-5492.

(15) Kurland, C. G., The RNA dreamtime. *BioEssays* **2010,** *32* (10), 866-871.

(16) Schwendinger, M. G.; Rode, B. M., Investigations on the mechanism of the salt-induced peptide formation. *Origins Life Evol. Biosphere* **1992,** *22* (6), 349-359.

(17) Schwendinger, M. G.; Tattler, R.; Saetia, S.; Liedl, K. R.; Kroemer, R. T.; Rode, B. M., Salt induced peptide formation: on the selectivity of the copper induced peptide formation under possible prebiotic conditions. *Inorg. Chim. Acta* **1995,** *228* (2), 207-214.

(18) Plankensteiner, K.; Righi, A.; Rode, B. M.; Gargallo, R.; Jaumot, J.; Tauler, R., Indications towards a stereoselectivity of the salt-induced peptide formation reaction. *Inorg. Chim. Acta* **2004,** *357* (3), 649-656.

(19) Li, F.; Fitz, D.; Fraser, D.; Rode, B., Arginine in the salt-induced peptide formation reaction: enantioselectivity facilitated by glycine, l- and d-histidine. *Amino Acids* **2010,** *39* (2), 579-585.

(20) Le Son, H.; Suwannachot, Y.; Bujdak, J.; Rode, B. M., Salt-induced peptide formation from amino acids in the presence of clays and related catalysts. *Inorg. Chim. Acta* **1998,** *272* (1-2), 89-94.

(21) Bujdák, J.; Rode, B. M., Silica, Alumina, and Clay-Catalyzed Alanine Peptide Bond Formation. *J. Mol. Evol.* **1997,** *45* (5), 457-466.
(22) Bujdák, J.; Rode, B. M., The effect of clay structure on peptide bond formation catalysis. *J. Mol. Catal. A: Chem.* **1999,** *144* (1), 129-136.
(23) Lambert, J.-F., Adsorption and Polymerization of Amino Acids on Mineral Surfaces: A Review. *Orig Life Evol Biosph* **2008,** *38* (3), 211-242.
(24) Lambert, J.-F.; Stievano, L.; Lopes, I.; Gharsallah, M.; Piao, L., The fate of amino acids adsorbed on mineral matter. *Planetary and Space Science* **2009,** *57* (4), 460-467.
(25) Meng, M.; Stievano, L.; Lambert, J.-F., Adsorption and Thermal Condensation Mechanisms of Amino Acids on Oxide Supports. 1. Glycine on Silica. *Langmuir* **2004,** *20* (3), 914-923.
(26) Guo, C.; Holland, G. P., Alanine Adsorption and Thermal Condensation at the Interface of Fumed Silica Nanoparticles: A Solid-State NMR Investigation. *The Journal of Physical Chemistry C* **2015,** *119* (45), 25663-25672.
(27) Shanker, U.; Bhushan, B.; Bhattacharjee, G.; Kamaluddin, Oligomerization of Glycine and Alanine Catalyzed by Iron Oxides: Implications for Prebiotic Chemistry. *Origins of Life and Evolution of Biospheres* **2012,** *42* (1), 31-45.
(28) Martra, G.; Deiana, C.; Sakhno, Y.; Barberis, I.; Fabbiani, M.; Pazzi, M.; Vincenti, M., The Formation and Self-Assembly of Long Prebiotic Oligomers Produced by the Condensation of Unactivated Amino Acids on Oxide Surfaces. *Angew. Chem. Int. Ed.* **2014,** *53* (18), 4671-4674.
(29) Fox, S. W.; Harada, K., The Thermal Copolymerization of Amino Acids Common to Protein1. *J. Am. Chem. Soc.* **1960,** *82* (14), 3745-3751.
(30) Søndergaard, J.; Asmund, G.; Larsen, M. M., Trace elements determination in seawater by ICP-MS with on-line pre-concentration on a Chelex-100 column using a 'standard' instrument setup. *MethodsX* **2015,** *2*, 323-330.
(31) Ochiai, E.-I., The evolution of the environment and its influence on the evolution of life. *Origins Life Evol Biosphere* **1978,** *9* (2), 81-91.
(32) Ochiai, E.-I., Copper and the biological evolution. *Biosystems* **1983,** *16* (2), 81-86.
(33) Rode, B. M.; Schwendinger, M. G., Copper-catalyzed amino acid condensation in water — A simple possible way of prebiotic peptide formation. *Origins Life Evol. Biosphere* **1990,** *20* (5), 401-410.
(34) Saetia, S.; Liedl, K. R.; Eder, A. H.; Rode, B. M., Evaporation cycle experiments — A simulation of salt-induced peptide synthesis under possible prebiotic conditions. *Origins Life Evol Biosphere* **1993,** *23* (3), 167-176.
(35) Russell, M. J., The Importance of Being Alkaline. *Science* **2003,** *302* (5645), 580-581.
(36) Kelley, D. S.; Karson, J. A.; Früh-Green, G. L.; Yoerger, D. R.; Shank, T. M.; Butterfield, D. A.; Hayes, J. M.; Schrenk, M. O.; Olson, E. J.; Proskurowski, G.; Jakuba, M.; Bradley, A.; Larson, B.; Ludwig, K.; Glickson, D.; Buckman, K.; Bradley, A. S.; Brazelton, W. J.; Roe, K.; Elend, M. J.; Delacour, A.; Bernasconi, S. M.; Lilley, M. D.; Baross, J. A.; Summons, R. E.; Sylva, S. P., A Serpentinite-Hosted Ecosystem: The Lost City Hydrothermal Field. *Science* **2005,** *307* (5714), 1428-1434.
(37) Russell, M. J.; Nitschke, W., Methane: Fuel or Exhaust at the Emergence of Life? *Astrobiology* **2017,** *17* (10), 1053-1066.
(38) Wong, M. L.; Charnay, B. D.; Gao, P.; Yung, Y. L.; Russell, M. J., Nitrogen Oxides in Early Earth's Atmosphere as Electron Acceptors for Life's Emergence. *Astrobiology* **2017,** *17* (10), 975-983.
(39) Stüeken, E. E.; Buick, R.; Schauer, A. J., Nitrogen isotope evidence for alkaline lakes on late Archean continents. *Earth. Planet. Sci. Lett.* **2015,** *411* (0), 1-10.

(40) Jones, B. E.; Grant, W. D.; Duckworth, A. W.; Owenson, G. G., Microbial diversity of soda lakes. *Extremophiles* **1998,** *2* (3), 191-200.
(41) Ferris, J. P.; Hagan Jr, W. J., HCN and chemical evolution: The possible role of cyano compounds in prebiotic synthesis. *Tetrahedron* **1984,** *40* (7), 1093-1120.
(42) Hanczyc, M. M.; Fujikawa, S. M.; Szostak, J. W., Experimental Models of Primitive Cellular Compartments: Encapsulation, Growth, and Division. *Science* **2003,** *302* (5645), 618-622.
(43) Macleod, G.; McKeown, C.; Hall, A.; Russell, M., Hydrothermal and oceanic pH conditions of possible relevance to the origin of life. *Origins Life Evol. Biosphere* **1994,** *24* (1), 19-41.
(44) Lafay, R.; Montes-Hernandez, G.; Janots, E.; Chiriac, R.; Findling, N.; Toche, F., Mineral replacement rate of olivine by chrysotile and brucite under high alkaline conditions. *J. Cryst. Growth* **2012,** *347* (1), 62-72.
(45) Catti, M.; Ferraris, G.; Hull, S.; Pavese, A., Static compression and H disorder in brucite, $Mg(OH)_2$, to 11 GPa: a powder neutron diffraction study. *Phys. Chem. Miner.* **1995,** *22* (3), 200-206.
(46) Brindley, G. W.; Kao, C.-C., Structural and IR relations among brucite-like divalent metal hydroxides. *Phys. Chem. Miner.* **1984,** *10* (4), 187-191.
(47) Brindley, G. W.; Kikkawa, S.; , A crystal-chemical study of Mg, Al and Ni, Al hydroxyperchlorates and hydroxy-carbonates. *Am. Mineral.* **1979,** *64*, 836-843
(48) Gregoire, B.; Ruby, C.; Carteret, C., Hydrolysis of mixed Ni^{2+}-Fe^{3+} and Mg^{2+}-Fe^{3+} solutions and mechanism of formation of layered double hydroxides. *Dalton Trans.* **2013,** *42* (44), 15687-15698.
(49) Boclair, J. W.; Braterman, P. S., Layered double hydroxide stability. 1. Relative stabilities of layered double hydroxides and their simple counterparts *Chem. Mater.* **1999,** *11* (2), 298-302.
(50) Cairns-Smith, A. G.; Hall, A.; Russell, M., Chapter 9 Mineral theories of the origin of life and an iron sulfide example. *Origins Life Evol. Biosphere* **1992,** *22* (1-4), 161-180.
(51) Arrhenius, G. O., Crystals and Life. *Helv. Chim. Acta* **2003,** *86* (5), 1569-1586.
(52) Anbar, A. D., Elements and Evolution. *Science* **2008,** *322* (5907), 1481-1483.
(53) Grégoire, B.; Erastova, V.; Geatches, D. L.; Clark, S. J.; Greenwell, H. C.; Fraser, D. G., Insights into the behaviour of biomolecules on the early Earth: The concentration of aspartate by layered double hydroxide minerals. *Geochim. Cosmochim. Acta* **2016,** *176*, 239-258.
(54) Erastova, V.; Degiacomi, M. T.; G. Fraser, D.; Greenwell, H. C., Mineral surface chemistry control for origin of prebiotic peptides. *Nature Communications* **2017,** *8* (1), 2033.
(55) Rozov, K.; Berner, U.; Taviot-Gueho, C.; Leroux, F.; Renaudin, G.; Kulik, D.; Diamond, L. W., Synthesis and characterization of the LDH hydrotalcite–pyroaurite solid-solution series. *Cem. Concr. Res.* **2010,** *40* (8), 1248-1254.
(56) Kasting, J. F., Earth's Early Atmosphere. *Science* **1993,** *259* (5097), 920-926.
(57) Grégoire, B.; Ruby, C.; Carteret, C., Structural Cohesion of M^{II}-M^{III} Layered Double Hydroxides Crystals: Electrostatic Forces and Cationic Polarizing Power. *Cryst. Growth Des.* **2012,** *12* (9), 4324-4333.
(58) Russell, M. J.; Hall, A. J.; Martin, W., Serpentinization as a source of energy at the origin of life. *Geobiology* **2010,** *8* (5), 355-371.
(59) Bellotto, M.; Rebours, B.; Clause, O.; Lynch, J.; Bazin, D.; Elkaïm, E., A reexamination of hydrotalcite crystal chemistry *J. Phys. Chem.* **1996,** *100* (20), 8527-8534.
(60) Thomas, G. S.; Rajamathi, M.; Kamath, P. V., DIFFaX Simulations of Polytypism and Disorder in Hydrotalcite. *Clays Clay Miner.* **2004,** *52* (6), 693-699.

(61) Britto, S.; Joseph, S.; Vishnu Kamath, P., Distinguishing crystallite size effects from those of structural disorder on the powder X-ray diffraction patterns of layered materials. *J. Chem. Sci.* **2010,** *122* (5), 751-756.

(62) Vieira, A. C.; Moreira, R. L.; Dias, A., Raman Scattering and Fourier Transform Infrared Spectroscopy of $Me_6Al_2(OH)_{16}Cl_2{\cdot}4H_2O$ (Me = Mg, Ni, Zn, Co, and Mn) and $Ca_2Al(OH)_6Cl{\cdot}2H_2O$ Hydrotalcites. *J. Phys. Chem. C* **2009,** *113* (30), 13358-13368.

(63) Kagunya, W.; Baddour-Hadjean, R.; Kooli, F.; Jones, W., Vibrational modes in layered double hydroxides and their calcined derivatives. *Chem. Phys.* **1998,** *236* (1–3), 225-234.

(64) Leroux, F.; Moujahid, E. M.; Roussel, H.; Flank, A.-M.; Briois, V.; Besse, J.-P., Local order of the transition metals for the substitution $(Co_{1-y}Cu_y)_2Al(OH)_6Cl{\cdot}nH_2O$ ($0<y<1$) in a Copper-Aluminium Layered Double Hydroxide-like phase. *Clays Clay Miner.* **2002,** *50* (2), 254-264.

(65) Rode, B. M.; Suwannachot, Y., The possible role of Cu(II) for the origin of life. *Coord. Chem. Rev.* **1999,** *190–192* (0), 1085-1099.

(66) Cadars, S.; Layrac, G.; Gerardin, C.; Deschamps, M.; Yates, J. R.; Tichit, D.; Massiot, D., Identification and quantification of defects in the cation ordering in Mg/Al layered double hydroxides. *Chem. Mater.* **2011,** *23*, 2821-2831.

(67) Rojas, R.; Barriga, C.; De Pauli, C. P.; Avena, M. J., Influence of carbonate intercalation in the surface-charging behavior of Zn-Cr layered double hydroxides. *Mater. Chem. Phys.* **2010,** *119* (1-2), 303-308.

(68) Rojas Delgado, R.; De Pauli, C. P.; Carrasco, C. B.; Avena, M. J., Influence of MII/MIII ratio in surface-charging behavior of Zn–Al layered double hydroxides. *Appl. Clay Sci.* **2008,** *40* (1-4), 27-37.

(69) Kosmulski, M., pH-dependent surface charging and points of zero charge. IV. Update and new approach. *J. Colloid Interface Sci.* **2009,** *337* (2), 439-448.

(70) Xu, Z. P.; Jin, Y.; Liu, S.; Hao, Z. P.; Lu, G. Q., Surface charging of layered double hydroxides during dynamic interactions of anions at the interfaces. *J. Colloid Interface Sci.* **2008,** *326* (2), 522-529.

(71) Fitz, D.; Jakschitz, T.; Rode, B. M., The catalytic effect of l- and d-histidine on alanine and lysine peptide formation. *J. Inorg. Biochem.* **2008,** *102* (12), 2097-2102.

FOR TOC ONLY

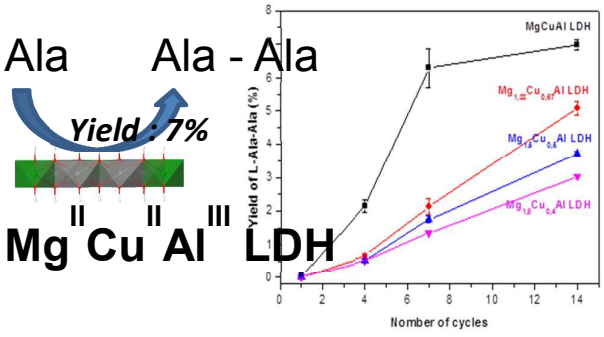

Peptide Formation on Layered Mineral Surfaces: The Key Role of Brucite-like Minerals on the Enhanced Formation of Alanine Dipeptides

B. Grégoire*,[a,c] H.C. Greenwell,[b] and Donald G. Fraser*,[a]

[a] Department of Earth Sciences, University of Oxford, South Parks Road, Oxford, OX1 3AN, United Kingdom.

[b] Department of Earth Sciences, Durham University, South Road, Durham, DH1 3LE United Kingdom.

[c] Université de Poitiers, CNRS, UMR 7285 IC2MP, 5 rue Albert Turpain, TSA 51106, 86073 Poitiers Cedex 9, France

E-mail : brian.gregoire@univ-poitiers.fr; don@earth.ox.ac.uk

Table ESI 1. Crystallographic parameters for prepared minerals used in the study.

LDH	Cell parameter (Å)		Apparent domain size (nm)	
	c (Å)	a (Å)	along [001]	along [110]
$Mg(OH)_2$	4.732	3.136	19.0	49.2
Mg_2Al LDH	22.684 (7.561)	3.037	7.9	23.6
Ni_2Al LDH	22.740 (7.580)	3.018	5.5	22.5
Zn_2Al LDH	22.670 (7.557)	3.068	20.5	43.5
Mg_3Al LDH	23.447 (7.816)	3.061	9.6	25.5

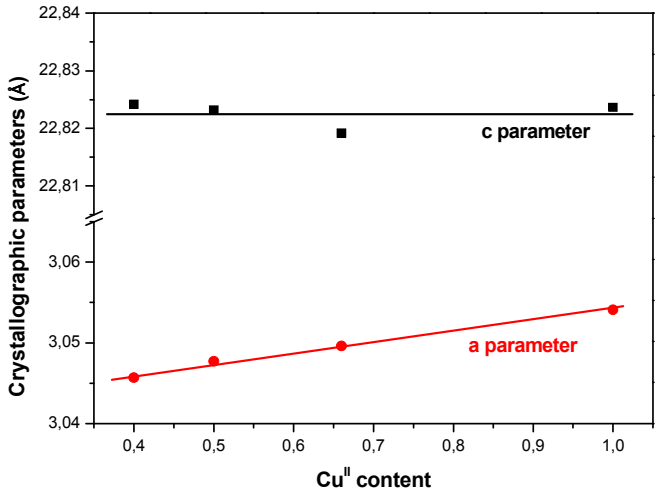

Figure ESI 1. Variation of the crystallographic cell parameters *a* and *c* as a function of Cu^{II} content within the layer of Ternary Mg/Cu/Al layered double hydroxides.

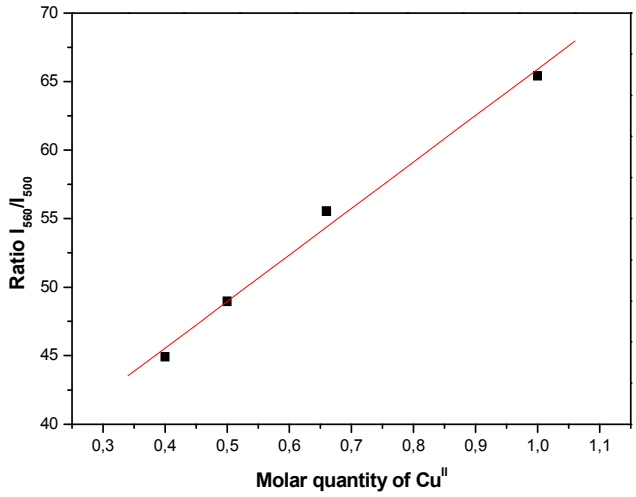

Figure ESI 2. Plotted variation in intensity of the Raman bands at 500 cm^{-1} and 560 cm^{-1} as a function of Cu content showing a linear correlation that can be used to assess the Cu content in Mg/Cu/Al LDH samples.

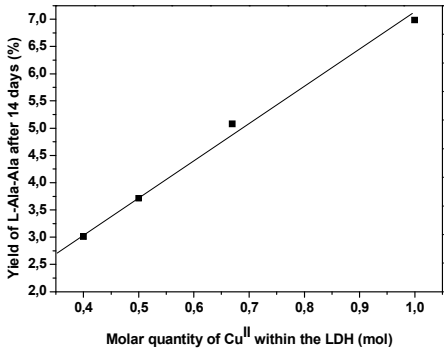

Figure ESI 3. Maximul yield from peptide forming reactions after 14 cycles on ternary Mg/Cu/Al layered double hydroxide minerals as a function of Cu^{II} content of the mienral.